INVERSE PROBLEM APPROACH FOR PARTICLE DIGITAL HOLOGRAPHY: PARTICLE DETECTION AND ACCURATE LOCATION

Ferréol Soulez[1,2]*, Loïc Denis*[1]*, Éric Thiébaut*[2]*, Corinne Fournier*[1]

[1]Laboratoire Hubert Curien (ex-LTSI) ; CNRS, UMR5516 ; Université Jean Monnet
18 rue Pr Benoît Lauras, F-42000 Saint-Etienne, France
[2]Université de Lyon, Lyon, F-69000, France ;
Université Lyon 1, Villeurbanne, F-69622, France ;
Centre de Recherche Astronomique de Lyon, Observatoire de Lyon,
9 avenue Charles André, Saint-Genis Laval cedex, F-69561, France ; CNRS, UMR 5574 ;
Ecole Normale Supérieure de Lyon, Lyon, France

ABSTRACT

Optical holography allows to record tridimensionnal informations of a scene using only one 2D sensor. Physical optics allows to analyticaly modelise hologram formation according to objects parameters (position, size, shape...). In simple objects case (*e.g.* spherical particles), the model is reduced to few parameters (four per particles: *x*,*y*,*z*,radius). Using inverse problem approach, it is possible to determine these parameters resolving a global optimization problem. This new approach is more efficient than classical method : particle parameters estimation is far more precise and it is possible to localize particles outside of the camera field of view. The presented method achieves to detect particles in an area sixteenth times wider than the CCD field of view with equal precision on both simulated and real digital holograms. Moreover strong improvements in the precision of the localization of the particles were noticed, particularly along the depth dimension.

1. INTRODUCTION

Particle image velocimetry (PIV) is a measurement technique for studying flows by retrieving velocimetry field from images of tracer particles in it. The development of optical holography applications in fluid mechanics [1, 2] have proven the capability of holography to give access to three dimensionnal distribution of micron-sized particles and their measurements. Bypassing the wet chemical processing, digital holography enable direct numerical processing by recording the hologram directly on a numerical detector. This allows fast acquisitions for high-speed phenomena analysis.

In-line holography is one of the most classical techniques in holography and the most efficient in digital holography for particle image velocimetry (DHPIV). In this simple setup every optical apparatus (laser, optics and camera) are aligned. Studied particles (water droplets) are illuminated with a laser collimated beam, and both object wave (scattered light) and reference wave (laser) are recorded on a digital camera. This setup is presented in figure 1.

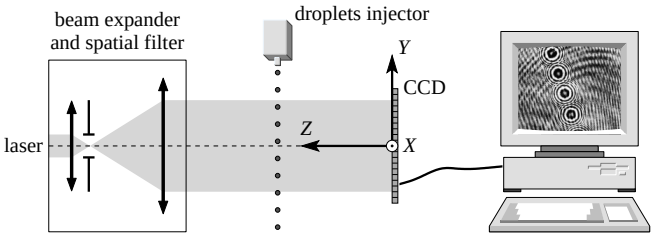

Fig. 1. In-line holography setup.

Over the past decade, many contributions have been made in the field of digital hologram processing in order to improve the measurement accuracy of the localization of micro-objects [3, 4]. The two main steps of the numerical processing are: a numerical reconstruction step to obtain a synthesized 3D distribution with focused particles, and a segmentation step to extract locations and sizes of the particles from this 3D distribution. Such approaches however suffer from various limitations:

- limited depth resolution (about 10 times worse than the transversal resolution),
- limited field of view (restricted to the center of the hologram to reduce the border effects)
- presence of spurious twin-images [5]
- multiple focusing [6]

In this paper, we propose a new approach using a inverse problem scheme. Bypassing numerical reconstruction and segmentation steps, our method allows to detect particles outside of the camera field of view with a fine precision. In this approach we search for the set of particle sizes and positions yielding a hologram model which best fits the real hologram image. For simple objects such as water droplets, physical optics allows to analytically model hologram formation according to objects parameters (four per particles: *x*,*y*,*z*,radius). Using inverse problem approach, it is possible

to determine these parameters resolving a global optimization problem. We effectively solve this global optimization problem by an iterative algorithm which alternates coarse detection of the particles and local optimization.

The paper is organized as follows. First, we recall the model of the hologram formation. Then we detail the principle of the proposed algorithm, in particular the detection and the local optimization stages. Finally, we apply our method to the reconstruction of holograms using both simulated and real world data. More details on the presented algorithm may be found in references [7] for local optimization stage.

2. MODEL OF THE HOLOGRAM IMAGE

We consider an incident beam of complex amplitude $\underline{A_0}$ which is diffracted by opaque spherical particles of radii r_j and coordinates (x_j, y_j, z_j). We work under Fresnel approximation, *i.e.* the distance z between a diffracting particle and the observation plane is such that [8] $z^3 \gg 4\pi r_j^4/\lambda$ achieved for $z \gtrsim 1\,\text{mm}$ when $r_j \approx 50\,\mu\text{m}$ is the largest particle's axis and $\lambda = 532\,\text{nm}$ is the laser wavelength. For spherical particles of radius r_j small enough to have $z_j \gg 4\,r_j^2/\lambda$, the complex amplitude $\underline{f_j}(x, y)$ of the wave diffracted by a single particle at coordinates (x_j, y_j, z_j) and observed at position $(x, y, z = 0)$ can be approximated by [9]:

$$\underline{f_j}(x,y) = \frac{r_j}{2\,\mathrm{i}\,\rho_j(x,y)}\,\mathrm{J}_1\!\left(\frac{2\,\pi\,r_j\,\rho_j(x,y)}{\lambda\,z_j}\right)\exp\!\left(\mathrm{i}\,\frac{\pi\,\rho_j^2(x,y)}{\lambda\,z_j}\right) \tag{1}$$

where $\rho_j(x,y) = \sqrt{(x-x_j)^2 + (y-y_j)^2}$ is the distance between the point $(x, y, z = 0)$ of the observation plane and the projection $(x_j, y_j, z = 0)$ of the position of the j-th particle on the detector at $z = 0$ and J_1 is the first order Bessel function. Thus, for n particles of parameters $\{x_j, y_j, z_j, r_j; j = 1, \ldots, n\}$ the intensity measured by the detector at position (x, y) is given by:

$$\begin{aligned} I(x,y) \;=\; & \gamma\,\left|\underline{A_0}\right|^2 + I_{\text{bg}} - 2\,\gamma\,\left|\underline{A_0}\right|^2 \sum_{j=1}^{n} \eta_j\,\mathrm{Re}(\underline{f_j}(x,y)) \\ & + \gamma\,\left|\underline{A_0}\right|^2 \sum_{i=1}^{n}\sum_{j=1}^{n} \eta_i\,\underline{f_i}(x,y)\,\eta_j\,\underline{f_j^*}(x,y) \end{aligned} \tag{2}$$

where γ accounts for the quantum efficiency and the conversion factor of the detector whereas I_{bg} accounts for the detector background level and for other spurious emission sources if any. In first approximation, the second order terms (interferences) can be neglected and the intensity simplifies to:

$$I(x,y) = I_0 - \sum_{j=1}^{n} \alpha_j\,\mathrm{Re}(\underline{f_j}(x,y)) \tag{3}$$

where $\alpha_j = 2\,\gamma\,\left|\underline{A_0}\right|^2\,\eta_j$ and $I_0 = \gamma\,\left|\underline{A_0}\right|^2 + I_{\text{bg}}$ is the image level given by the detector illuminated by the laser without diffracting particles.

3. PRINCIPLE

Our algorithm is based on an inverse problem approach: we search for the set of particle sizes and positions yielding a hologram model which best fits the real hologram image. In other words, we need to find the optimal set of n particles of parameters $\{x_j, y_j, z_j, r_j; j = 1, \ldots, n\}$ that minimize the weighted least-squares penalty:

$$\mathcal{P}_n = \sum_{k=1}^{N_{\text{pixel}}} W_k\,\left[D_k - M_{n,k}\right]^2 \tag{4}$$

where D_k is the k-th pixel value of the observed hologram and $W_k = 1/\,\mathrm{Var}(D_k)$ is its statistical weight. The model $M_{n,k}$ for n particles is directly given by Eq. 3:

$$M_{n,k} = I_0 - \sum_{j=1}^{n} \alpha_j\,\mathrm{Re}(\underline{f_j}(X_k, Y_k))\,, \tag{5}$$

where (X_k, Y_k) are the coordinates of the k-th pixel.

Stated like this, the problem requires global optimization over the space of particle parameters. Such problem has numerous local minimum and can not be solved directly. We effectively solve this global optimization problem by an iterative algorithm which alternates coarse detection of the particles and local optimization as described in figure 2. At the

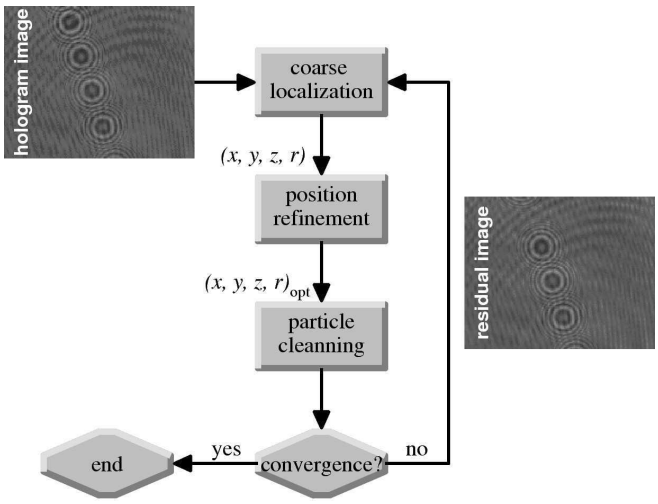

Fig. 2. Synopsis of the method.

n^{th} iteration of this algorithm, we minimize $\mathcal{P}_n$ with respect to the parameters $\{I_0, \alpha_n, x_n, y_n, z_n, r_n\}$ and consider the other particle parameters as fixed. Our misfit criterion then reads:

$$\mathcal{P}_n = \sum_{k=1}^{N_{\text{pixel}}} W_k\,\left[R_{n-1,k} - I_0 + \alpha_n\,\mathrm{Re}(\underline{f_j}(X_k, Y_k))\right]^2 . \tag{6}$$

$R_{n-1,k}$ is the residual image after having subtracted the contribution of the previous $n-1$ particles:

$$R_{n-1,k} = D_k + \sum_{j=1}^{n-1} \alpha_j\,\mathrm{Re}(\underline{f_j}(X_k, Y_k))\,, \tag{7}$$

where, of course, $R_{0,k} = D_k$.

Optimizing only on the new particle parameters rather than fitting all parameters for all particles yields a significant speed up in the algorithm. Moreover, since the signature of a given particle is severly disturbed by the patterns due to the other particles, we achieve an improved sensitivity to the detection and location of faint particle signatures, by such iterative processing over the residual images. A typical run of the algorithm on real data is shown by Fig. 3.

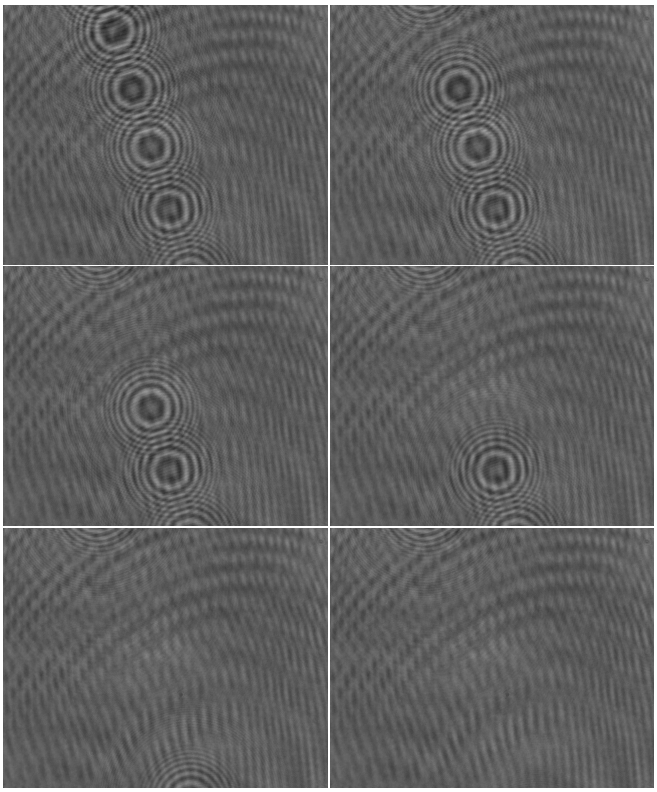

Fig. 3. Iterative particle removal in real hologram image. From top left to bottom: initial hologram image $R_0 = D$ and residual images R_1, R_2, R_3, R_4 and R_5 after detection and removal of 0, 1, 2, 3, 4 and 5 particles respectively.

3.1. Detection

At the n^{th} iteration of this algorithm, particle detection is done by estimating the vector of parameters $p_n = \{x_n, y_n, z_n, r_n\}$ that minimize $\mathcal{P}_n$. Using computationnal tricks, it is possible to rapidly evaluate $\mathcal{P}_n$ for the whole coarse discretized 4D grid of interest (x,y,z,r) using FFT. Detection takes 5 FFTs per (z, r) plane. A particle will be detected at the point where $\mathcal{P}_n$ is minimal.

Owing the large extension of a microparticle diffraction figure, particle outside of the camera transversal field of view. With formulation defined in Eq. 6, it is possible to explore outside of the field of view. $\mathcal{P}_n$ can be estimated over a work region bigger than the CCD. On this virtual sensor the residuals are defined by:

$$R'_{n-1,k} \equiv \begin{cases} R_{n-1,k}(x'_k, y'_k) & \text{inside the field of view,} \\ 0 & \text{outside the field of view,} \end{cases} \quad (8)$$

and corresponding weight map by:

$$W'_k \equiv \begin{cases} \text{Var}(D_k)^{-1} & \text{if } D_k \text{ is known} \\ 0 & \text{Otherwise} \end{cases} \quad (9)$$

If we consider noise as stationnary on the entire sensor $\text{Var}(D_k)$ becomes constant and W'_k can be viewed as a binary mask on the data. As a consequence, the effective field of view can be several times larger than the CCD (up to sixteenth times in our experiments).

3.2. Parameters refinement

The coarse parameters (x_n,y_n,z_n,r_n) from the detection stage can be refined by local optimisation [7]. This optimisation consists on minimizing $\mathcal{P}_n$ using a trust-region Newton algorithm [10]. Such an algorithm requires a local quadratic approximation of the penalty function $\mathcal{P}_n$ which is provided by the first and second order partial derivatives of the penalty with respect to the parameters. It leads to sub-pixels precision.

4. RESULTS

This method was applied to the reconstruction of holograms using both simulated and real world data. We first used simulated data to assess the actual performances of our algorithm under various conditions.

4.1. Simulation

To caracterize this algorithm we process several simulated holograms. The main goal of this test was to compare measurement errors on parameters of particle outside of the field of view versus inside the field of view. Every test were done with 100 particles. Such concentration represents standard conditions for a sufficently fast process of our algorithm. We consider three simulated hologram types with different radius range: one with radius between 3.5 and 5µm (we call it type I), another with radius between 30 and 40µm (type III) and a last one with intermediate radius between 15 and 20µm (type II). Every simulation were made for a 1024×1024 camera with square pixel of 6.70 µm width and a laser of 632.8*nm*. The particle are randomly distibuted in a box of $8.00 \times 8.00 \times 30.00\,mm$ located at about $250\,mm$ from the sensor. The resulting holograms were processed once with the full field of view (1024×1024 pixels) and once with a small field of view considering only the 512×512 pixels on its center. The error on the four parameters fitted in our model (position and radius) was evaluated. Rms error upon these parameters is shown in table 1.

This technique shows equal error (about 0.3 µm or 1/20 pixels) in lateral positionning (Δx and Δy) for every simulations. The

configuration FOV	type	Δx	Δy	Δz	Δr
1024	I	0.28	0.28	1.38	0.46
512	I	0.28	0.28	6.38	0.72
1024	II	0.28	0.28	2.53	0.03
512	II	0.28	0.28	11.8	0.09
1024	III	0.28	0.28	14.3	0.14
512	III	0.39	0.39	46.85	0.17

Table 1. Root mean squared errors for the estimated particles parameters in several simulation configurations —field of view (FOV) is 512×512 or 1024×1024, type I are for particles of size $3.5\,\mu\text{m} \leq r \leq 5\,\mu\text{m}$, type II for $15\,\mu\text{m} \leq r \leq 20\,\mu\text{m}$ and type III for $30\,\mu\text{m} \leq r \leq 40\,\mu\text{m}$.

high spatial frequency diffraction rings help to precisely locate the depth of the particles. Since these rings are attenuated as the size of the particles increases, the longitudinal errors are worse for bigger particles. On the other hand, this attenuation favors the determination of the particle radius.

4.2. Experimental data

We carried out an experimental test of our algorithm using real data from an in-line holography setup. The experimental layout is shown by Fig. 1 and the components are as follows:

The laser is a double cavity YAG (ULTRA-PIV 30, Quantel) with a 0.532 µm wavelength. It emits pulses of 7 ns short enough to freeze the droplets motion.

The injector is a piezoelectric device which generates monodisperse droplets. The droplet diameter is tunable from 50 µm to 100 µm. The injector can work in droplet-on-demand mode, generating droplets at constant time intervals (1000 Hz in the case of the considered data set).

The camera is a 12-bit CCD (PCO Sensicam) with 1280×1024 pixels of size $6.7\,\mu\text{m} \times 6.7\,\mu\text{m}$. The camera is at about 25 cm of the injector in order not to disturb the flow experiment. This leads to a small but realistic numerical aperture of $\Omega = 0.014$.

The experimental test data consists of a set of 200 holograms. The 3D positions and diameters of droplets were extracted from this data set by our algorithm. Figure 3 shows the residual images during the processing of one of the experimental hologram. Four or five particles can be seen on the CCD images. Our algorithm however detects up to 16 particles as shown in Fig. 4.

The measured particles positions are shown in Fig. 5. Clearly the average trajectory of the particles is a straight line as can be expected from the experimental conditions and particle's spacing follows ballistic trajectory. At each extremity of the jet reconstruction, some depth miss estimation can be contated. It is mainly due to slight divergence of laser beam that lead to non-modelized diffraction pattern deformation which

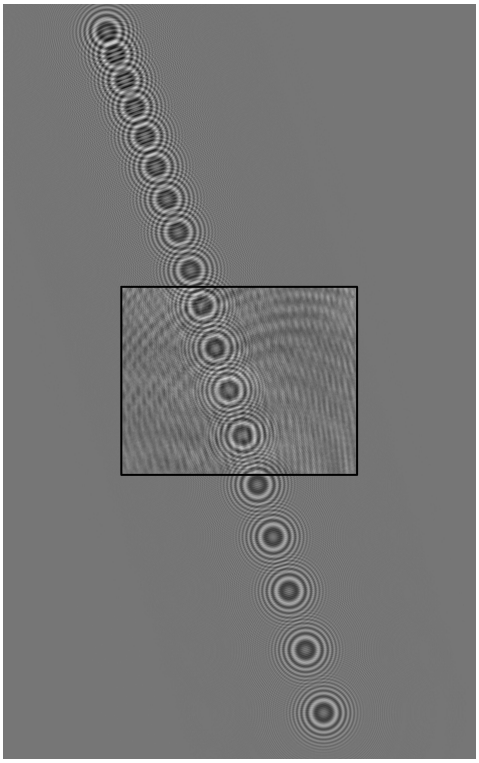

Fig. 4. Superposition of a real hologram (in the box) with the model synthetised with the 18 detected particles by the algorithm (14 are outside of the field of view)

grows as the particle is far from the center of the CCD. The other observed deviations from the ideal straight trajectory are mostly due to real physical effects. Indeed the oscillations and the beam divergence which can be seen in Fig. 5 are due to vibrations of the injector. Hence the effective precision of the measured positions is smaller than the variations due to these physical effects.

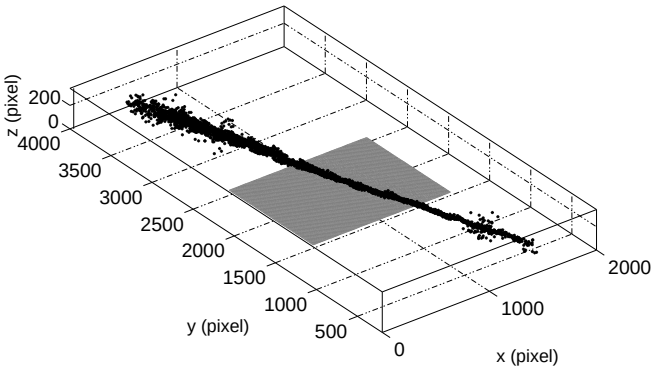

Fig. 5. Droplets jet reconstruction. 3D representation of segmented droplets. Grey area represents camera field of view.

The droplet sizes estimated by our algorithm have a bell-shaped distribution (see Fig. 6) with a mean diameter of 94.1 µm and a standard deviation of 0.3 µm in agreement with the settings of the droplet injector.

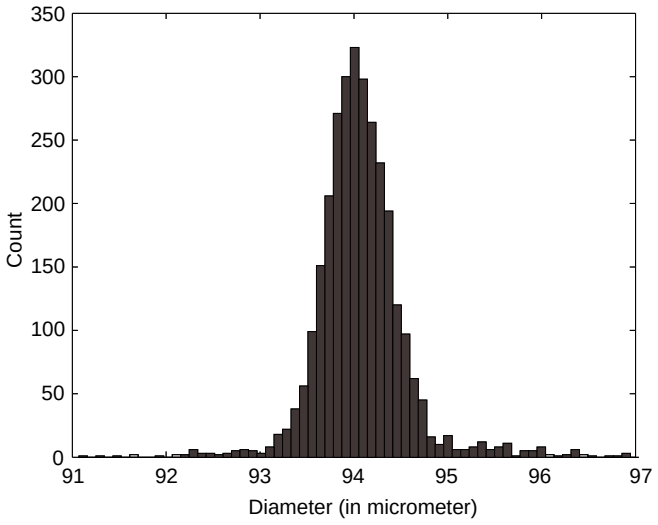

Fig. 6. Measured diameters histogram

The processing time scales as the number of particles per hologram image. For the present experiments, with a Pentium IV CPU 3.60 GHz with 2 GBytes of RAM our algorithm took 7 minutes per particle: 4 minutes for the detection and 3 minutes for particle parameters refinement. We plan to greatly reduce this time by performing multiple detections per pass of our iterative algorithm. We also expect a speedup by a factor of roughly two thanks to trivial computational optimizations such as using faster numerical routines to compute the Bessel functions.

5. CONCLUSION

In this paper we describe a new algorithm for the detection and localization of particles in digital holography. The most important difference with other existing techniques is that our processing is based on an inverse problem approach and does not require any direct inversion. In this framework, we introduce a simplified model of the hologram images which depends on the sizes and positions of the diffracting particles. We then solve the problem by seeking for the set of particle parameters for which the difference between the model and the data is statistically minimal. Such a criterion turns out to have multiple local minima and thus global optimization is required to properly solve the problem. Our algorithm effectively achieves the global minimum by performing an approximative detection of the particles in the whole parameter space followed by a local refinement of the parameters. By repeating these steps on the residual images, obtained by subtracting the model to the data, our algorithm is able to detect particles even the ones which have a faint signature compared to the diffraction pattern due to the other particles.

As estimation is done in data space, our algorithm does suffer from data truncation and can account for bad data or non-rectangular holograms by setting to zero the weights of bad pixels or pixels outside the area covered by the detector. It allows to detect particles outside from the sensor.

We have tested our algorithm on simulated and real data. Our results show that the precision along the depth direction is largely improved and is much better than the optical resolution in such conditions ($\delta z \geq \lambda/\Omega^2 = 2.6\,\mathrm{mm}$). When dealing with real data, it appears that our algorithm is also robust with respect to non-homogeneous illumination and to spurious patterns as the CCD fringes which can be seen in the 5th residual image of Fig. 3. Moreover, this figure show that, even only one particle signature can be seen, our algorithm is able to detect 13 more particles, integrating informations spread all over the sensor.

6. REFERENCES

[1] C. S. Vikram, "Holographic particle diagnostics," in *SPIE Milestone*, 1990, vol. MS21.

[2] K. D. Hinsch, "Holographic particle image velocimetry," *Measurement Science and Technology*, vol. 13, pp. R61–R72, 2002.

[3] T. M. Kreis, M. Adams, and W. Jüptner, "Methods of digital holography: A comparison," Munich, Germany, 1997, SPIE.

[4] K. D. Hinsch and S. F. Herrmann, "Special issue : Holographic particle image velocimetry," *Measurement Science & Technology*, vol. 15, 2004.

[5] L. Denis, C. Fournier, T. Fournel, and C. Ducottet, "Twin-image noise reduction by phase retrieval in in-line digital holography," in *Wavelets XI*, Manos Papadakis, Andrew F. Laine, and Michael A. Unser, Eds., San Diego, CA, USA, 2005, vol. 5914, pp. 148–161, Proceedings of the SPIE.

[6] C. Fournier, C. Ducottet, and T. Fournel, "Digital in-line holography: influence of the reconstruction function on the axial profile of a reconstructed particle image," *Measurement Science & Technology*, vol. 15, pp. 686–693, 2004.

[7] F. Soulez, L. Denis, C. Fournier, E. Thiébaut, and C. Goepfert, "Inverse problem approach for particle digital holography: accurate location based on local optimisation," *J. Opt. Soc. Am. A*, vol. 24, april 2007.

[8] J. W. Goodman, *Introduction to Fourier Optics*, Mc Graw-Hill, 1996.

[9] G. A. Tayler and B. J. Thompson, "Fraunhofer holography applied to particle size analysis: a reassessment," *Opt. Acta.*, vol. 23, pp. 261–304, 1976.

[10] Jorge J. Moré and Danny C. Sorensen, "Computing a trust region step," *SIAM J. Sci. Stat. Comp.*, vol. 4, no. 3, pp. 553–572, 1983.